

Investigations into the Relationship between Spheromak, Solar, and Astrophysical Plasmas

EX/P4-22

P. M. Bellan, S. C. Hsu, J. F. Hansen, M. Tokman, S. E. Pracko, C. A. Romero-Talamas

Caltech, Pasadena CA 91125, USA,
e-mail contact of main author: pbellan@its.caltech.edu

Abstract. Spheromaks offer the potential for a simple, low cost fusion reactor and involve physics similar to certain solar and astrophysical phenomena. A program to improve understanding of spheromaks by exploiting this relationship is underway using (i) a planar spheromak gun and (ii) a solar prominence simulator. These devices differ in symmetry but both involve spheromak technology whereby high-voltage is applied across electrodes linking a bias magnetic flux created by external coils. The planar spheromak gun consists of a co-planar disk and annulus linked by a poloidal bias field. Application of high voltage across the gap between disk and annulus drives a current along the bias field. If the current to flux ratio exceeds the inverse of the characteristic linear dimension, a spheromak is ejected. A distinct kink forms just below the ejection threshold. The solar simulation gun consists of two adjacent electromagnets which generate a “horse-shoe” arched bias field. A current is driven along this arched field by a capacitor bank. The current channel first undergoes pinching, then writhes, and finally bulges outwards due to the hoop force.

1. Planar spheromak gun

The planar spheromak gun [1, 2] is designed to have the simplest possible geometrical configuration consistent with DC helicity injection. The gun, shown in Fig. 1, consists of a 20.3 cm diameter copper disk inner electrode surrounded by a coplanar copper annulus outer electrode (21 cm inside diameter, 50.8 cm outside diameter) and is mounted on the end of a cylindrical vacuum chamber. A coil located immediately behind the gap between the disk and annulus creates a bias vacuum poloidal magnetic field linking the disk and annulus. This system is topologically equivalent to previously used coaxial magnetized plasma guns but differs by having coplanar electrodes rather than coaxial cylinder electrodes. High speed gas puff valves eject hydrogen or argon through 8 nozzles on the disk and 8 nozzles on the annulus. A 60 μF ignitron-switched low-inductance capacitor bank charged to approximately -5 kV is applied to the disk and the annulus is connected to machine ground. The high voltage breaks down the gas and drives up to 150 kA from disk to annulus.

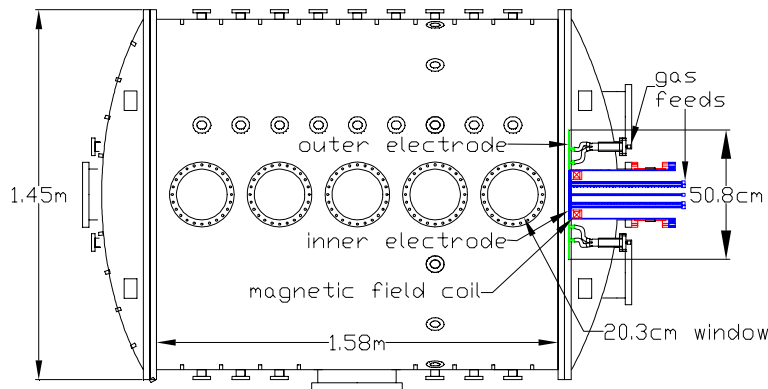


Figure 1:

An important initial result of this experiment is the observation that the gas injection arrangement is important. When gas is injected from the disk only, breakdown is exceedingly difficult but when gas is injected from disk and annulus, breakdown is straightforward and highly reproducible. Photographs of

the breakdown show that the initial plasma consists of well-defined discrete, filamentary current channels that start at a disk gas injection port and then follow the vacuum magnetic field to a corresponding annulus injection port. Thus, at breakdown, eight arched current channels appear, each spanning an anode-cathode pair of gas ports. A few microseconds after formation the disk ends of the eight discrete current channels coalesce to form a single central current channel which is bright, discrete, and has a radius which increases with increasing distance from the disk. The annulus ends of the current channels also coalesce to form a dimmer, more diffuse umbrella-shaped return current shroud.

The central column then lengthens, becomes jet-like, and at a critical value of gun current, develops a very distinct helical instability as shown in Fig. 2. Measurements of the current channel dimensions, the current, and estimates of the strength of the embedded poloidal field indicate that this growing helix is a Kruskal-Shafranov kink which destabilizes when the current channel attains a critical axial length. The parameters for kink onset also constitute the threshold for spheromak formation. For currents exceeding the value at which this kinking occurs, photographs indicate that the plasma detaches from the gun and flies off. Magnetic probe measurements indicate that the detached plasma is a spheromak, i.e., has closed poloidal flux surfaces which link a magnetic axis.

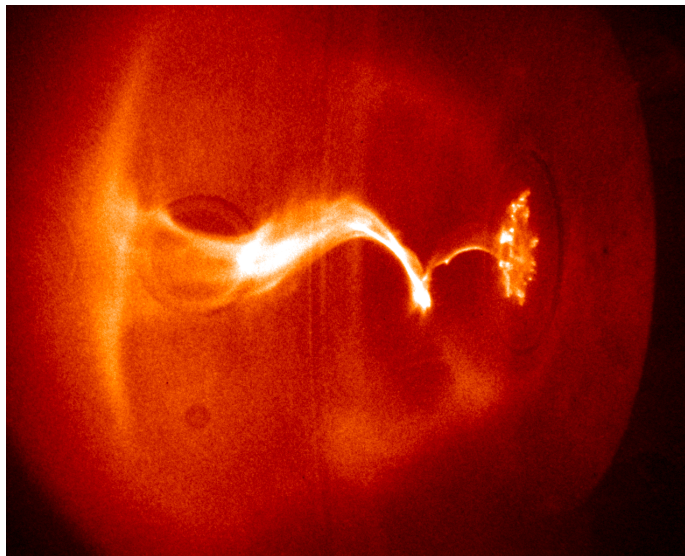


Figure 2:

These results indicate that spheromak formation is, not surprisingly, associated with a substantial departure from axisymmetry. The spheromak formation criterion $\lambda_{gun} > \lambda_{geom}$ with $\lambda_{gun} = \mu_0 I / \psi$ and $\lambda_{geom} = 1/L$ where L is a characteristic length, is equivalent within a geometrical factor of order unity to the Kruskal-Shafranov condition for kink instability, i.e., $B_\theta L / B_z \pi a > 1$. Here a is the current channel radius, L is the current channel length, $B_\theta = \mu_0 I / 2\pi a$, and $\psi = B_z \pi a^2$. The jetting behavior of the central current channel suggests a mass flow associated with spheromak formation. That is, the spheromak does not just “form” in a pre-existing background plasma, but rather the same MHD forces which distend and twist magnetic fields also convect plasma from the gun.

The jetting of plasma from the gun is reminiscent of the astrophysical jets spawned by rotating accretion disks[3]. This similarity is more than coincidental because the planar spheromak gun provides an excellent replica of the field topology of a rotating accretion disk. This is because an accretion disk rotating with azimuthal velocity U_θ and linking a poloidal field $B_z(r)$ produces a radial electric field $E_r = -U_\theta B_z$ which drives current along the poloidal field. By comparison, the capacitor bank in the lab experiment directly applies a radial electric field along the poloidal field linking the disk to the annulus. The jetting behavior can be interpreted in several ways. The simplest is to consider that there is an unbalanced magnetic pressure associated with the non-uniformity of the toroidal field and that this magnetic pressure distends the poloidal field. The jetting is constrained by the field line tension of the stretched poloidal magnetic

field so the jet velocity is some fraction of the Alfvén velocity. The jet convects plasma away from the gun electrode. An equivalent point of view is that the jet is accelerated by unbalanced $J_r B_\phi = -\partial/\partial z (B_\phi^2/2\mu_0)$ forces.

This jet behavior has implications for more general situations because it suggests that magnetized plasma jets [4] could develop at any surface that (i) provides a gas source, (ii) intercepts field lines, and (iii) has a voltage drop along the intercepted field lines. An important example would be the situation of tokamak or RFP error field lines that intercept a gas-loaded wall. An EMF applied along such an error field (e.g., by an Ohmic heating transformer) would cause plasma jets to be accelerated inwards from the wall into the interior following the error field line flux tube.

Argon plasmas have been used for laser induced fluorescence (LIF) studies in this device. Preliminary LIF measurements of the argon ion distribution function indicate a 20-40 eV ion temperature. The LIF system consists of a YAG-pumped narrow-band tunable dye laser. The ion distribution is determined by scanning the dye laser for successive plasma shots and measuring the fluorescent signal using a fast photomultiplier.

2. High speed photography of SSPX plasmas

A high speed camera system has been installed on the SSPX spheromak experiment at the Lawrence Livermore National Lab. Optical access was difficult on SSPX because its 1 m diameter flux conserver is located inside a much larger vacuum tank and the flux conserver has only a narrow gap for viewing. A re-entrant cavity was constructed with a lens located immediately outside the flux conserver gap and then a system of relay lenses was used to transfer the image back to a camera located external to the vacuum chamber. This arrangement allows viewing nearly the entire flux conserver interior with the camera located 50 cm away from the flux conserver.

The camera has the capability to take two successive frames with interframe interval less than 1 μ s. This provides the opportunity to determine the direction and speed of moving structures. Photographs of the initial formation stages are clearest and show (i) a shroud of plasma blowing out of the region between inner and outer spheromak electrodes, (ii) formation of a central column, (iii) rotation of this central column, and (iv) formation of a spheromak-like vortex as the tip of this central column folds back. This sequence takes place during the first 100 μ s of the discharge and is quite reproducible. This behavior is similar to the planar spheromak gun, except that the presence of the flux conserver acts as a barrier to the unbounded expansion observed in the planar spheromak gun. There is preliminary evidence of a correlation between voltage spikes and column compression. A typical photo of the central column is shown in Fig.3. After the formation stage, the flux conserver fills up with the plasma, the hydrogen “burns through”, and it becomes difficult to discern shapes because distinct edges no longer exist.

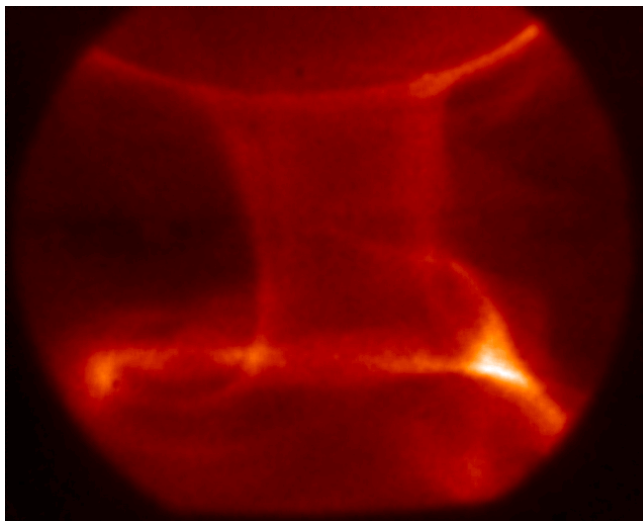


Figure 3:

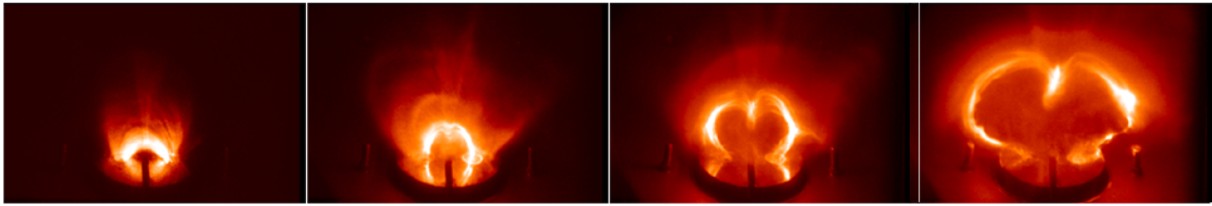


Figure 4: Typical observed sequence of operation of solar prominence simulation plasma.

3. Simulation of solar prominence eruptions using spheromak technology

The solar plasma gun [5] was designed to simulate solar prominence eruptions, but its operation also provides insights regarding wall-intercepting error fields that might occur in toroidal confinement devices. This is because the solar prominence gun can be considered as a finite-length flux tube which intercepts a wall at two points and which also has an EMF driving current along the axis of the flux tube. The operation sequence is similar to the planar spheromak gun, the main difference being the non-coaxial geometry. Various MHD forces are clearly evident in the sequence of operation. Initially, the magnetic field is a vacuum field produced by a pair of bias coils. This field is an arched field that links two electrodes. Hydrogen gas is injected into the region between the two electrodes and a large EMF is applied across the electrodes using a $30 \mu\text{F}$ capacitor bank ($\leq 80 \text{ kA}$, $\leq 6 \text{ kV}$). The gas breaks down, forming an arch-shaped plasma. The plasma starts with the shape of the vacuum magnetic field, but very quickly pinches so that the flux tube becomes axially uniform. The arched flux tube then twists, writhes about its axis, and often breaks up into smaller filaments. The major radius of the axis then expands due to the hoop force. The pinching, twisting, kinking, and hoop expansion can all be clearly distinguished as seen in Fig.4. Hoop expansion has been inhibited [5] by applying an external magnetic field which plays the role of the vertical magnetic field of a tokamak. The entire experiment duration is about $10 \mu\text{s}$ and the characteristic time for significant evolution is about $1 \mu\text{s}$.

Like the planar spheromak gun, the operation of the solar gun is quite sensitive to the details of gas injection. Consistent breakdown is only obtained when gas is injected from both anode and cathode. No breakdown occurs when gas is injected from anode only, and a delayed breakdown occurs when gas is injected from the cathode only. In the cathode-only gas injection situation, high speed photography shows that the arc starts at the cathode and then propagates towards the anode, the propagation time being a few microseconds. When gas is injected from both cathode and anode, breakdown occurs in about $0.1 \mu\text{s}$. The solar gun behavior also suggests the existence of some kind of pumping process which transports plasma axially along the flux tube, filling up the flux tube.

4. Differential Tensioning/Detensioning of Magnetic Fields

A 3D numerical MHD code was used to model [6] a solar MHD configuration (coronal mass ejection) which has topology analogous to a 180° toroidal segment of a tokamak. This configuration involves twisting of magnetic fields which then bifurcate into a system of flux tubes having distinct topology. The bifurcation is related to the curvature of a magnetic axis. The boundary condition for the system consists of a plane penetrated by an arched magnetic field (like the vacuum toroidal field of a 180° toroidal segment of a tokamak) as shown in Fig.5. The magnetic field lines intercepting the plane are arranged to co-rotate by imposition of electric fields in the plane; these electric fields are oriented in the direction corresponding to the minor radius of a tokamak. The co-rotation twists up the magnetic field about a magnetic axis (dotted line in figure). The line between the centers of the two vortices defines the y -axis.

The twisted fields are observed to bifurcate such that the fields inboard of the magnetic axis behave differently from those which are outboard. The inboard fields (darker shade in Fig.5) are stretched and descend as if they are under increased tension. In contrast, the outboard fields (lighter shade in Fig.5) have a rigid rotor deformation and move upwards, behaving as if they are detensioned (loosened). This separation of the inboard and outboard fields from each other in the vicinity of the magnetic axis results in a reduction of field intensity at the magnetic axis. The reason why the inboard fields stretch whereas

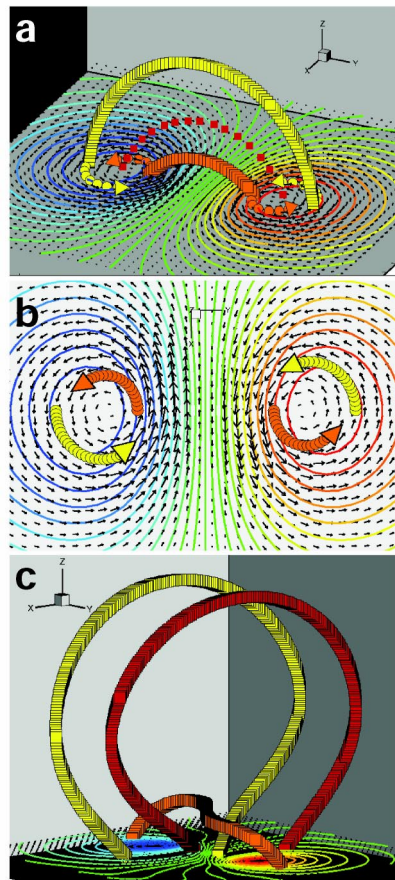


Figure 5:

the outboard fields rigidly rotate can be seen by examining the co-rotating vortices shown in Fig.5(b). The co-rotation causes the footpoints (places where field lines intercept the base plane) of the inboard field lines to separate from each other in both the x and the y directions, thereby stretching this field line. In contrast, co-rotation of the outboard field lines causes the ends of these field lines to separate in the x direction, but approach each other in the y direction. Figures 5(b) and (c) show this effect. Deviations from axisymmetry occur in a tokamak could result in a similar unraveling of the inner and outboard portions of field lines.

References

- [1] HSU S.C., BELLAN P.M., “A laboratory plasma experiment for studying magnetic dynamics of accretion discs and jets”, *Monthly Notices Royal Astronom. Soc.* **334** (2002) 257.
- [2] HSU S.C., BELLAN P.M., “Study of magnetic helicity injection via plasma imaging using a high-speed digital camera”, *IEEE Trans. Plasma Sci.* **30**, Part 1 (2002) 10
- [3] LOVELACE, R. V. E., “Dynamo model of double radio-sources”, *Nature* **262** (1976) 649.
- [4] BELLAN, P.M., “Vorticity model of flow driven by purely poloidal currents”, *Phys. Rev. Lett* **69** (1992) 3515
- [5] HANSEN, J.F., BELLAN, P.M., “Experimental demonstration of how strapping fields can inhibit solar prominence eruptions”, *Astrophysical J.* **563** (2001) L183
- [6] TOKMAN, M., BELLAN, P.M., “Three-dimensional model of the structure and evolution of coronal mass ejections”, *Astrophysical J.* **567** (2002) 1202